A general approach to site-specific antibody drug conjugates

Feng Tian[a,1], Yingchun Lu[a], Anthony Manibusan[a], Aaron Sellers[a], Hon Tran[a,2], Ying Sun[a], Trung Phuong[a], Richard Barnett[a], Brad Hehli[a], Frank Song[a], Michael J. DeGuzman[b], Semsi Ensari[b,3], Jason K. Pinkstaff[c], Lorraine M. Sullivan[c], Sandra L. Biroc[c], Ho Cho[d], Peter G. Schultz[e,1], John DiJoseph[f], Maureen Dougher[f], Dangshe Ma[f], Russell Dushin[g], Mauricio Leal[h], Lioudmila Tchistiakova[i], Eric Feyfant[i,4], Hans-Peter Gerber[f], and Puja Sapra[f,1]

[a]EuCode Technology, Ambrx, Inc., La Jolla, CA 92037; [b]CMC Department and [c]Preclinical Science, [d]Ambrx, Inc., La Jolla, CA 92037; [e]Department of Chemistry and Skaggs Institute for Chemical Biology, The Scripps Research Institute, La Jolla, CA 92037; [f]Oncology Research Unit and [h]Pharmacokinetics, Dynamics and Metabolism, Pfizer, Inc., Pearl River, NY 10965; [g]Worldwide Medicinal Chemistry, Pfizer, Inc., Groton, CT 06340; and [i]Global BioTherapeutic Technologies, Pfizer, Inc., Cambridge, MA 02140

Contributed by Peter G. Schultz, December 10, 2013 (sent for review October 1, 2013)

Using an expanded genetic code, antibodies with site-specifically incorporated nonnative amino acids were produced in stable cell lines derived from a CHO cell line with titers over 1 g/L. Using anti-5T4 and anti-Her2 antibodies as model systems, site-specific antibody drug conjugates (NDCs) were produced, via oxime bond formation between ketones on the side chain of the incorporated nonnative amino acid and hydroxylamine functionalized monomethyl auristatin D with either protease-cleavable or noncleavable linkers. When noncleavable linkers were used, these conjugates were highly stable and displayed improved in vitro efficacy as well as in vivo efficacy and pharmacokinetic stability in rodent models relative to conventional antibody drug conjugates conjugated through either engineered surface-exposed or reduced interchain disulfide bond cysteine residues. The advantages of the oxime-bonded, site-specific NDCs were even more apparent when low–antigen-expressing (2+) target cell lines were used in the comparative studies. NDCs generated with protease-cleavable linkers demonstrated that the site of conjugation had a significant impact on the stability of these rationally designed prodrug linkers. In a single-dose rat toxicology study, a site-specific anti-Her2 NDC was well tolerated at dose levels up to 90 mg/kg. These experiments support the notion that chemically defined antibody conjugates can be synthesized in commercially relevant yields and can lead to antibody drug conjugates with improved properties relative to the heterogeneous conjugates formed by nonspecific chemical modification.

Antibody drug conjugates (ADCs) are emerging as a new class of anticancer therapeutics that combine the efficacy of small-molecule therapeutics with the targeting ability of an antibody (Ab) (1, 2). By combining these two components into a single molecular entity, highly cytotoxic small-molecule drugs (SMDs) can be delivered to cancerous target tissues, thereby enhancing efficacy while reducing the potential systemic toxic side effects of the SMD. Conventional ADCs are typically produced by conjugating the SMD to the Ab through the side chains of either surface-exposed lysines or free cysteines generated through reduction of interchain disulfide bonds (3, 4). Because antibodies contain many lysine and cysteine residues, conventional conjugation typically produces heterogeneous mixtures that present challenges with respect to analytical characterization and manufacturing. Furthermore, the individual constituents of these mixtures exhibit different pharmacology with respect to their pharmacokinetic, efficacy, and safety profiles, hindering a rational approach to optimizing this modality (5).

Recently, it was reported that the pharmacological profile of ADCs may be improved by applying site-specific conjugation technologies that make use of surface-exposed cysteine residues engineered into antibodies (THIOMABS) that are then conjugated to the SMD, resulting in site-specifically conjugated ADCs (TDCs) with defined Ab–drug ratios. Relative to the heterogeneous mixtures created using conventional conjugation methodologies, site-specifically conjugated TDCs demonstrated equivalent in vivo potency, improved PK, and an expanded therapeutic window (6, 7). Although this approach may be useful for generating site-specifically conjugated ADCs, THIOMABS produced using this process are not directly amenable to conjugation, but instead, require a multistep process that includes decapping of the engineered cysteine residues, which inevitably results in the partial breaking and reformation of structurally important internal disulfide bonds. Site-specific ADCs generated by enzymatic modification also have demonstrated improved stability and pharmacokinetics; however, a surface-exposed transglutamase tag (LLQG) needs to be engineered into antibodies at a permissive site (8).

To provide a more facile and generally applicable approach for synthesizing site-specifically conjugated ADCs, we developed a recombinant DNA-based eukaryotic protein expression system using Chinese hamster ovary (CHO) cells to biosynthetically incorporate nonnative amino acids into a given Ab scaffold (9). Nonnative amino acids, such as *para*-acetylphenylalanine (*p*AF) and *para*-azidophenylalanine (*p*AZ), can provide orthogonal conjugation chemistries that otherwise are not available from functional groups present in the 20 canonical amino acids. Nonnative amino acid incorporation technology using *Escherichia coli* expression systems can provide large quantities (>5 g/L) of proteins for clinical use (10). However, *E. coli* expression is limited to relatively

Significance

Here we demonstrate the ability to genetically incorporate nonnative amino acids into proteins in mammalian cells using both transient and stable platform expression systems that provide yields and fidelities compatible with commercial applications. To illustrate the utility of this methodology we have generated chemically homogeneous antibody drug conjugates (NDCs) with precise control over the site and stoichiometry of drug conjugation. In rodent xenograft models these NDCs display improved properties, including half-life, efficacy and safety, relative to conventional heterogeneous ADCs. These advances allow the generation of therapeutic antibody drug conjugates with medicinal chemistry like control over structure, which should greatly facilitate the optimization of their pharmacological activities.

Author contributions: F.T., H.C., P.G.S., H.-P.G., and P.S. designed research; F.T., Y.L., A.M., A.S., H.T., Y.S., T.P., R.B., B.H., F.S., M.J.D., S.E., J.K.P., L.M.S., S.L.B., J.D., M.D., R.D., M.L., L.T., and E.F. performed research; F.T., Y.S., and R.B. contributed new reagents/analytic tools; F.T., Y.L., A.S., J.K.P., L.M.S., S.L.B., P.G.S., J.D., D.M., L.T., and P.S. analyzed data; and F.T., P.G.S., and P.S. wrote the paper.

The authors declare no conflict of interest.

[1]To whom correspondence may be addressed. E-mail: feng.tian@ambrx.com, schultz@scripps.edu, or puja.sapra@pfizer.com.

[2]Present address: Eli Lilly & Company, Applied Molecular Evolution, San Diego, CA 92121.

[3]Present address: Science and Engineering, Genentech, Inc., Oceanside, CA 92056.

[4]Present address: Schrodinger Biologics, Cambridge, MA 02142.

This article contains supporting information online at www.pnas.org/lookup/suppl/doi:10.1073/pnas.1321237111/-/DCSupplemental.

simple, nonglycosylated proteins. The production of more complex glycosylated proteins, such as full-length antibodies, requires a eukaryotic expression system such as CHO cells. Previous attempts to incorporate nonnative amino acids in eukaryotic organisms have met with limited success as the product titers achieved were not high enough for product development and commercialization (11, 12).

We report here, the development of a stable expression system using CHO cells (EuCODE) that produces antibodies incorporating nonnative amino acids with titers over 1 g/L. We have applied this technology to the generation of site-specific Ab drug conjugates (NDCs) synthesized by site-specific coupling of the potent tubulin inhibitor, monomethyl auristatin D (MMAD) (13), to genetically encoded *p*AF residues in anti-5T4 (A1) and anti-Her2 (Her) antibodies. 5T4, also known as trophoblast glycoprotein, is a cell surface antigen that internalizes rapidly, and is highly expressed on colorectal and gastric cancers (14). Human epidermal growth factor receptor 2 (Her2) is the target of the therapeutic agents Trastuzumab and Trastuzumab-mcc-DM1 (T-DM1), and is highly expressed in breast cancers (15). The resulting NDCs were compared in rodent efficacy studies to both conventional ADCs (generated from reduced interchain cysteines) and engineered cysteine TDCs. The NDCs demonstrated superior efficacy and pharmacokinetic properties, and in a single-dose rat toxicology study, the anti-Her2 NDC was well tolerated at dose up to 90 mg/kg. Finally, in vitro plasma stability studies showed that the site of conjugation had a significant impact on the stability of rationally designed cleavable linkers.

Results and Discussion

EuCODE Technology in CHO cells. To develop a commercially viable Ab production system in mammalian cells for the generation of NDCs, we used an engineered *E. coli*-derived tyrosyl-tRNA/aminoacyl-tRNA synthetase orthogonal pair and amber nonsense codon (TAG) for the specific incorporation of nonnative amino acids into antibodies (16, 17). Unlike *E. coli*, where the amber codon is the least used among the three nonsense codons and rarely terminates essential genes (18), eukaryotic cells such as CHO use all three codons (TAG, TAA, TGA) with nearly equal frequency and uniform distribution throughout their genomes (19). Given the long production times required when using CHO cells (a few weeks vs. only a few days in *E. coli*), it has been commonly assumed that the universal elongation of TAG-terminated host cell proteins would negatively impact the vitality and productivity of the host CHO cell. To overcome this issue, we created a CHO platform cell line from CHO K1 (ATCC), in which the engineered orthogonal tyrosyl-tRNA (20) and aminoacyl-tRNA synthetase were stably integrated into the CHO K1 genome. This platform cell line was used for stable cell line generation for Ab production. To ensure high level expression of the orthogonal amber suppressor tRNA, we created a vector (*p*AF-tRNA) that encoded up to 40 copies of $tRNA_{CUA}$ whose expression was driven by an internal promoter sequence. A second vector (*p*AF-RS) was generated that encodes the *p*AF-RS gene, codon optimized for CHO expression, whose expression was driven by a CMV promoter. The *p*AF-RS vector was electroporated into CHO K1 cells to generate a RS stable pool under the selective pressure of zeocin. The orthogonal tRNA vector was then electroporated into the RS stable pool to generate a tRNA/RS stable pool under the selective pressure of puromycin. The tRNA/RS stable pool was enriched by FACS sorting using transient expression of a mutant GFP gene as a marker. An amber codon was engineered at residue position 56 of the GFP gene expressed under a CMV promoter on a transient vector and was transfected into the tRNA/RS stable pool. In a single cell, the full-length GFP was expressed only in the presence of nonnative amino acid and with the stable expression of both $tRNA_{CUA}$ and *p*AF-RS. Following a single-cell isolation step from the FACS-enriched tRNA/RS stable pool, we suspension-adapted the adherent stable cell line into serum-free medium EX302 and obtained a platform CHO cell line, 4E2. This cell line was found to be stable in cell culture for over a month as measured by the transient expression titers of an amber-human growth hormone mutant. The genomic DNA of 4E2 was isolated and characterized by GFP-specific PCR confirming that no GFP vector was stably integrated into the genome of 4E2.

From the platform cell line 4E2, first-generation stable cell lines expressing the mutant Ab A1 HC-A114*p*AF (Scheme S1) (Kabat numbering) were generated using Lonza's GS Ab expression system (21) with a methionine sulfoximine (MSX) concentration of 50 μM. The stable cell lines were further amplified/subcloned at 250 μM MSX to isolate second-generation stable cell lines. The second-generation stable cell line, which underwent fed-batch evaluation, yielded Ab titers in excess of 1 g/L in the presence of 1 mM *p*AF in 30-mL shake flasks (Fig. 1*B*). At the end of the fed-batch process, cell viability remained over 75%, consistent with a process that can be used to support clinical scale production and eventual commercialization (Fig. 1*A*). It should also be noted that the peak cell densities achieved thus far are only around 7×10^6 cells per mL. Compared with current industry standards for Ab manufacturing where peak cell densities routinely exceed 1.5×10^7 cells per mL, we believe there is still opportunity, through media and process optimization, to further increase nonnative amino acid-containing Ab titers well beyond 1 g/L. The current fed-batch process was successfully scaled in a 5-L bioreactor (Fig. 1 *A* and *B*). Furthermore, with the stable cell line expression system, in the absence of *p*AF, no full-length Ab titers were detectable. In addition, due to incomplete Amber suppression efficiency, we expected that early termination of heavy-chain translation would result in the accumulation of some N-terminal truncation products. By positioning the amber mutation proximal to the N terminus, the full-length product can be purified using a single protein A chromatography step because the early truncation product does not bind to protein A (Fig. S1*A*).

To demonstrate the robustness of this product-specific stable cell generation system, we generated stable cell lines for a number of antibodies, including anti-5T4, anti-EGFR, anti-Her2, and anti-PMSA full-length antibodies. The colony formation numbers and the shape of the Ab titer distribution curves among these clones are consistent, and similar to, standard WT Ab clone generation. Multiple nonnative amino acid-containing Ab titers have exceeded 1 g/L in fed-batch processes without requiring extensive process and media development. The stability of an anti-Her2 Ab producing stable clone was determined to exceed 60 generations of culture passage based on full-length Ab titers obtained in a 7-d batch culture. In addition to the incorporation of *p*AF, stable cell lines that incorporate *p*AZ have also been generated, thereby extending orthogonal site-specific conjugation to 2+3 "click" chemistry (22). We do not yet fully understand how EuCODE stable cell lines can deliver high Ab productivity while at the same time maintaining high cell viability, but we hypothesize that the stably expressed tyrosyl-tRNA/RS intracellular concentrations were optimized during our cell line development process to balance amber suppression efficiency and cell viability.

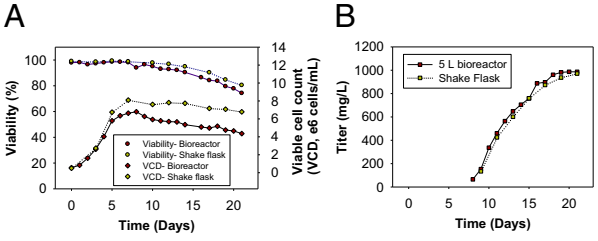

Fig. 1. Fed-batch cell culture results of A1 HC-S115*p*AF stable cell line. (*A*) Growth profile in shake flask and 5-L bioreactor. (*B*) Titer (in milligrams per liter) in shake flask and 5-L bioreactor.

For research quantities of mutant antibodies, stable pools expressing the Ab of interest were generated from the platform cell line 4E2. In the presence of 100 μM MSX, bulk stable Ab mutant titers up to 60 mg/L were achieved. Where transient Ab expression was desired, Ab expression was accomplished using the FreeStyle CHO-S system, a vector that encodes $tRNA_{CUA}$, *p*AF-RS, Ab heavy- and light-chain genes, and media supplemented with *p*AF (1–4 mM). In the presence of *p*AF, Ab titers of up to 10 mg/L have been obtained with this production system.

Syntheses of ADCs. The Ab purification and conjugation process for making NDCs is simple and robust. Nonnative amino acid-containing full-length antibodies (IgG1) were purified from cell culture medium on a protein A column followed by cation exchange column chromatography. Similar to WT antibodies, typical purification yields were over 90%. These antibodies were conjugated to SMDs derivatized with short "noncleavable" PEG linkers containing a terminal alkoxyamine (NC-D1) (Scheme 1 and Scheme S2). At pH 4.0, the alkoxyamine functional group reacts with the aromatic ketone on *p*AF to form an oxime bond that is stable under physiological conditions (10). The residual SMD was removed by ultrafiltration to yield nearly homogenous NDCs with two drugs per Ab. The overall conjugation yield was over 95%.

The mutant Ab A1 HC-S115*p*AF and the corresponding NC-D1 conjugate were analyzed by RP-HPLC in both nonreduced and reduced forms to assess conjugate purity and to confirm heavy-chain specificity (Fig. S1 *B* and *C*). The chromatogram of the nonreduced form shows a single main peak eluting at 8.2 min. Upon conjugation, the retention time of the main peak shifts to 11 min, consistent with the formation of a single conjugated species. Peak integration of the RP-HPLC chromatogram indicated that the Ab conjugate is ~98% pure (Fig. S1*B*). Analysis of the reduced A1 HC-S115*p*AF NC-D1 conjugate compared with native or mutant Ab shows a shift in retention time for the heavy chain peak, whereas the retention time of the light chain remained unchanged (Fig. S1*C*). Thus, the RP-HPLC data confirm that conjugation of NC-D1 occurs specifically on the heavy chain and largely leads to the production of a single species. A shoulder peak on the reduced heavy chain was observed preconjugation and postconjugation. Mass spectrometry analysis of the shoulder and main peaks appeared to be comparable and this shoulder was determined to be a hydrophilic variant (likely different glycosylation forms), not a result of the conjugation.

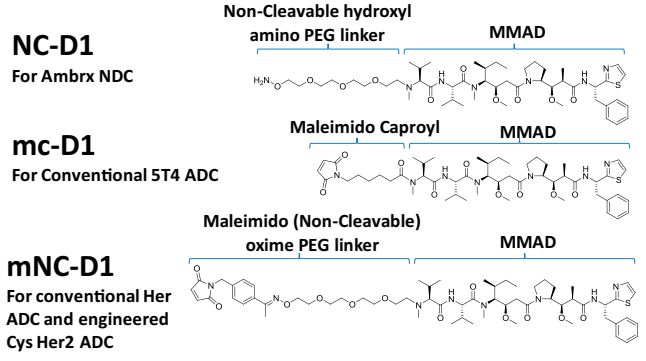

Scheme 1. Drug and linkers used in efficacy studies. A noncleavable linker with MMAD (NC-D1) was used in synthesizing site-specific NDCs (A1 HC-S115*p*AF-NC-D1 and Her HC-A114*p*AF-NC-D1). Linker mc-D1 was used to synthesize conventional anti-5T4 ADC (A1 mc-D1) by conjugation through interchain cysteines. mNC-D1 was used to synthesize anti-Her2 Ab conventional drug conjugate (Her mNC-D1) and a site-specifically engineered cysteine-containing ADC (Her HC-A114C-mNC-D1). The resulting drug loading per Ab was around 4:1 and 2:1 for conventional conjugations and site-specific conjugates, respectively.

Intact mass analysis of the reduced and deglycosylated WT A1, A1 HC-S115*p*AF, and A1 HC-S115*p*AF-NC-D1 exhibited mass shifts consistent with a single substitution of *p*AF for a serine residue as well as a single SMD-linker conjugated to the *p*AF-containing heavy chain (Fig. S2). To further evaluate the specificity of *p*AF incorporation and site-specific conjugation, trypsin digests of the samples were analyzed by liquid chromatography and tandem mass spectrometry with MS^2 enabled (LC/MS/MS). The UV (214 nm) profiles show an absence of the WT T11 peptide at 46.3 min with a new peak at 50.2 min. Upon conjugation, the peak further shifts to the right to 60.2 min. MS/MS analysis of these new peaks confirmed *p*AF incorporation at the site HC-S115 in the variant and efficient and complete conjugation of NC-D1 to the two *p*AF residues in the variant (Fig. S3).

The ketone group of *p*AF, which is incorporated into antibodies at a 2:1 amino acid-to-Ab ratio, selectively reacts with alkoxyamine groups appended to the SMD. The selectivity of the reaction ensures a drug-to-Ab ratio (DAR) of 2 even in the presence of severalfold molar excess of SMDs, and following prolonged reaction times. The orthogonal conjugation chemistry precludes the possibility of overconjugation, which may create unwanted higher DAR species, which is inevitable for ADCs created using conventional conjugation methods (23, 24). Others have previously reported that ADCs with a DAR of 2 display an improved therapeutic window compared with higher drug-loaded ADC species that tend to have poor pharmaceutical properties and may be associated with significant toxicities (5).

Potent and Selective in Vitro Cytotoxic Activities. To compare the cytotoxic activity of site-specific A1 HC-S115*p*AF-NC-D1 with conventional ADCs, A1 mc-D1 was created by chemical modification of reduced interchain disulfide bonds. The SMD used for this conventional conjugation approach has a maleimido caproyl (mc) noncleavable linker (Scheme 1). An average DAR of ~4.0 for A1 mc-D1 was determined by MS. The cytotoxic activity of site-specific A1 HC-S115*p*AF-NC-D1 and conventional A1 mc-D1 were evaluated on two 5T4-positive cell lines, MDAMB435/5T4 and MDAMB468, and a 5T4-negative cell line, Raji. The IC_{50} values are listed (Table S1). Even with a twofold difference in drug loading (4.0 for A1 mc-D1 and 2.0 for A1 HC-S115*p*AF-NC-D1), nearly equivalent potencies (IC_{50} values of 56 and 44 ng/mL, respectively) were measured for these two conjugates when evaluated on MDAMB435/5T4 cells. In the low–5T4-expressing cell line, MDAMB468, A1 HC-S115*p*AF-NC-D1 is twofold more potent than conventional A1 mc-D1. The significant difference in the in vitro potency between 3+ (MDA MB435/5T4, cells expressing high levels of 5T4) and 2+ (MDA MB468, endogenously expressed 5T4) is likely due to different levels of 5T4 expression in the two cell lines (25).

To further explore the potency of the NDCs, we compared the cytotoxicity of anti-Her2 Ab-derived NDC (HC-A114*p*AF) with a conventional ADC (again generated by modification of interchain disulfide bonds) and with a THIOMAB generated from a site-specifically engineered cysteine (HC-A114C) in the anti-Her2 Ab, TDC (6). To minimize the structural differences in the different conjugate formats, we used 1-(4-acetylbenzyl)-1*H*-pyrrole-2,5-dione as the spacer element to closely emulate the oxime linkage present in the *p*AF-based oxime conjugates, while also providing a maleimido handle for conjugation to the cysteine residues (mNC-D1) in both conventional ADC and TDC conjugates (Scheme 1). The DARs of NDC (Her HC-A114*p*AF-NC-D1), conventional ADC (Her mNC-D1), and TDC format (Her HC-A114C-mNC-D1) were 2.0, 4.5, and 2.3, respectively (Table S2). Antigen-binding sites of HCC1954, N87, BT474-M1, and MDAMB361DYT2 were determined by flow cytometry to be 6.68×10^5, 4.60×10^5, 4.04×10^5, and 1.52×10^5, respectively (Fig. S4). The cytotoxic activity of these three anti-Her2 Ab conjugates [site-specific NDC (Her HC-A114*p*AF-NC-D1), conventional (Her mNC-D1), and site-specific cysteine (Her HC-A114C-mNC-D1)] were evaluated on four endogenous Her2-positive cell lines (HCC1954, N87,

BT474-M1, and MDAMB361DYT2) and a Her2-negative cell line (MDAMB468) (Fig. S5). From the IC_{50} values (Table S2), it is apparent that the NDC (Her HC-A114*p*AF-NC-D1) is ~1.2- to 12-fold more potent than the conventional conjugate, Her mNC-D1, on these cells even with the drug loading on NDC (Her HC-A114*p*AF-NC-D1) being twofold less than the drug loading on conventional conjugate (Her mNC-D1). Furthermore, nonspecific cytotoxicity of Her HC-A114*p*AF-NC-D1 on Her2-negative cells, MDAMB468, is approximately eightfold less than that of conventional Her mNC-D1 on the same cell line. Interestingly, the engineered cysteine site-specific ADC, Her HC A114C-mNC-D1, which is also a near two-drug loaded conjugate, appeared to be less potent than the conventional conjugate (Her mNC-D1) (IC_{50} values of 18 vs. 9.5 ng/mL, respectively, on HCC1954 cells, and 1,552 vs. 570 ng/mL, respectively, on MDAMB361DYT2 cells). These data, especially with low antigen expressing (2+) cell lines, demonstrate that the site-specific NDC (Her HC-A114*p*AF-NC-D1) is the most potent and selective conjugate among the site-specific *p*AF (NDC), conventional, and site-specific cysteine (TDC) conjugates evaluated. The improved in vitro efficacy and selectivity of NDCs may derive from a combination of the superior stability of the oxime linkage before internalization and more efficient intracellular drug release within the endosome/lysosome after internalization. More investigation is warranted to fully understand the mechanism behind these findings and whether structural effects on the Ab surface play a role in the difference between Her HC-A114*p*AF-NC-D1 and Her HC A114C-mNC-D1 (26).

Nonnative Amino Acid Conjugates Demonstrate Superior in Vivo Efficacy Compared with the Conventional or a Site-Specific Cysteine-Derived Conjugate. To determine whether NDCs have enhanced efficacies in vivo, A1 HC-S115*p*AF-NC-D1 and Her HC-A114*p*AF-NC-D1 were evaluated in several in vivo xenograft studies and compared with conjugates created via conventional conjugation or site-specifically engineered cysteine conjugation. The ADCs were administrated to mice bearing s.c. tumor xenografts established from cancer cell lines. In the case of the anti-5T4 example, A1 HC-S115*p*AF-NC-D1 and A1 mc-D1 were evaluated in two different models, MDAMB435/5T4 (Fig. 2 *A* and *B*) and MDAMB361DYT2 (Fig. S6 *A* and *B*) xenograft models, which have different levels of 5T4 expression. Animals were treated with A1 mc-D1 and A1 HC-S115*p*AF-NC-D1 i.v. at 1, 3, and 10 mg/kg Q4dx4 starting on day 1. As shown (Fig. 2 *A* and *B* and Fig. S6 *A* and *B*), dose-dependent antitumor activity of A1 mc-D1 and A1 HC-S115*p*AF-NC-D1 was demonstrated in two models. Although A1 mc-D1 displayed limited in vivo efficacy, A1 HC-S115*p*AF-NC-D1 was highly efficacious and caused complete regression of tumor growth in 8 of 8 mice and in 10 of 10 mice treated at 10 mg/kg in MDAMB435/5T4 and MDAMB361DYT2 tumor models, respectively. Furthermore, all animals treated at 10 mg/kg appeared to be tumor free—no evidence of tumors was present during gross pathology examination at the termination of the study, except in the case of one animal that had a single small tumor of 44 mm^3 at the end of the experiment in the MDAMB361DYT2 model. For the 3 mg/kg treatment group in MDAMB361DYT2, there were 5 of 10 animals without evidence of disease, and 4 of 5 animals with remaining measurable tumors had reduced tumor size compared with the initial tumor volume at the end of the experiment. Similarly, two of eight animals treated at 3 mg/kg in the MDAMB435/5T4 model had no measurable tumors.

Even more potent in vivo activities were observed with the anti-Her2 example using Her HC-A114*p*AF-NC-D1 in two xenograft models, MDAMB361DYT2 and HCC1954 (Fig. S6 *C* and *D*). In these studies, Her HC-A114*p*AF-NC-D1 completely inhibited tumor growth in 8 of 10 animals treated at 1 mg/kg, and in all 10 animals treated at both 3 and 10 mg/kg in the MDAMB361DYT2 model. In the HCC1954 xenograft model, treatment at 3 mg/kg with Her HC-A114*p*AF-NC-D1 caused complete regression of tumor growth in all eight treated mice. In addition, six of eight animals treated at 1 mg/kg had no evidence of tumors at termination of the study. These promising results led us to directly compare Her HC-A114*p*AF-NC-D1 to conventional Her mNC-D1 and to cysteine site-specific conjugate Her HC-A114*p*AF-mNC-D1 at 1 mg/kg in two xenograft models, MDAMB361DYT2 and HCC1954. As shown in Fig. 2 *C* and *D*, for animals treated at 1 mg/kg Q4dx4, Her HC-A114*p*AF-NC-D1 was the most efficacious (values of $P < 0.005$ for comparison against Her HC-A114C-mNC-D1 on day 13 and beyond in the HCC1954 model, and day 33 and beyond in the MDAMB361-DYT2 model, and for Her mNC-D1 on day 35 and beyond in the HCC1954 model). The results also showed that the conventional Her mNC-D-1 was more potent than Her HC-A114C-mNC-D1 in both models tested (values of $P < 0.005$ for comparison against Her HC-A114C-mNC-D1 on day 13–16 in the HCC1954 model, and on day 41 and beyond in the MDAMB361DYT2 model). Additionally, all three ADCs caused complete regression of tumor growth in all animals treated at 3 mg/kg, with no statistical difference among the groups.

Therefore, we conclude that even though NCDs have fewer drugs per antibody, they display superior in vivo efficacy in rodent models compared to conventional conjugates which have twice the drug load. Furthermore, these NDCs are more efficacious than corresponding site-specific engineered cysteine conjugates containing a comparable drug load and a similar linkage.

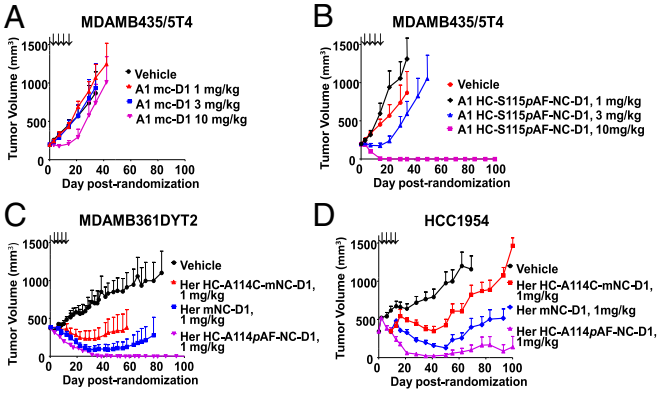

Fig. 2. Nonnative amino acid site-specific conjugates display superior in vivo efficacy compared with conventional and site-specific cysteine conjugates dosed on days 1, 5, 9, and 13. (*A* and *B*) In vivo efficacy determination of A1 mc-D1 and A1HC-S115*p*AF-NC-D1 in 5T4-positive tumor models of MDAMB435/5T4 at 1, 3, and 10 mg/kg. (*C* and *D*) Comparison of Her HC-A114*p*AF-NC-D1 conjugate with Her mNC-D1 and Her HC-A114C-mNC-D1 in two Her2-positive tumor models of MDAMB361DYT2 and HCC1954 at 1 mg/kg.

NDCs Demonstrate Superior Pharmacokinetics. Pharmacokinetic analysis was performed in mice treated with a single 3 mg/kg dose of WT A1 Ab, conventional A1 mc-D1 conjugate, *p*AF-containing Ab alone, or its NC-D1 conjugate in the anti-5T4 example. As shown in Fig. 3, systemic exposure of the A1 HC-S115*p*AF-NC-D1 was similar to that of the WT A1 Ab. Ab exposure of the A1 HC-S115*p*AF-NC-D1 was unexpectedly higher than the nonconjugated A1 HC-S115*p*AF-variant Ab ($P = 0.0056$). Surprised by this finding, we repeated the experiment and obtained the same results. Furthermore, we measured FcRn and albumin binding and observed no difference in binding affinities between the NDC and unconjugated Ab. The percentage exposure of NDC/total Ab for A1 HC-S115*p*AF-NC-D1 was ~85%. This indicates that the conjugate remains mostly intact over the course of 14 d. This is a significant improvement compared with conventional A1 mc-D1 and site-specific cysteine conjugates reported in the literature (6, 15). We believe the improved PK of NDCs may be attributable to the intrinsic chemical stability of the oxime conjugation chemistry as well as improved homogeneity and the absence of fast-clearing higher DAR species.

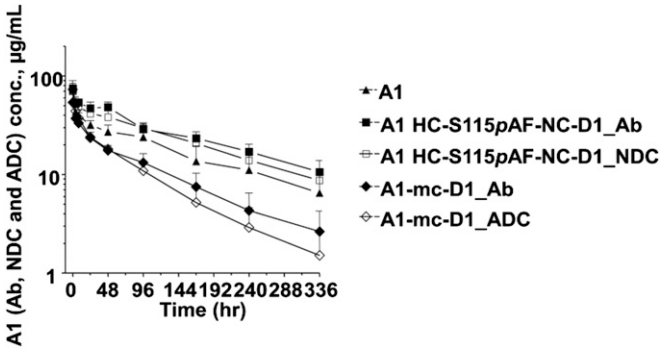

Fig. 3. Pharmacokinetics of Ab A1 and its conjugates A1 HC-S115*p*AF-NC-D1 and A1-mc-D1 over 14 d in mice dosed i.v. with 3 mg Ab/kg (single dose). For the conjugates, the total Ab (Ab with or without drug, A1 HC-S115*p*AF-NC-D1_Ab, or A1-mc-D1_Ab), NDC (A1 HC-S115*p*AF-NC-D1), and ADC (A1-mc-D1_ADC) were determined.

The PK study of the anti-5T4 Ab, ADC, and NDC collectively revealed that the improved in vivo efficacy of NDCs may be due to the much improved pharmacokinetics relative to the corresponding conventional ADC. It has been previously reported that ADCs created via conventional conjugation methodologies have a shorter half-life and lower overall exposure than their corresponding WT antibodies (27). In contrast, our anti-5T4 NDC had a PK that was equal to or slightly better than the WT Ab. The anti-drug ELISA also confirmed that the oxime linkage between the SMD and Ab is highly stable in vivo—a significant improvement relative to conventional maleimido linkages that have been reported to be chemically unstable in plasma (26, 28).

Plasma Stability of NDCs with Cleavable Linkers. To demonstrate that the site of conjugation matters, we created NDCs with cleavable linkers. These linkers, such as the valine–citrulline–*p*-aminobenzyloxycarbonyl (PABC) linker, have been widely used in ADC designs. After the ADCs are internalized into the cancer cells, the valine–citrulline dipeptide is readily cleaved in the lysosome by the protease cathepsin B. Following elimination of the PABC spacer, free drug is released inside the cell (23). Cleavable linkers provide an intracellular SMD release mechanism after internalization that does not require total lysosomal Ab degradation when a more stable noncleavable linker is used. However, when cleavable linkers are used, the stability of the linker in physiological environments has been a concern. Premature linker cleavage before internalization into cancer cell results in unwanted systemic toxicity (29). To determine whether the conjugation site affects the stability of the valine–citrulline–PABC drug linker, HC-D1 and SHC-D1 were conjugated to A1-HC-A114*p*AF or A1 HC-S115*p*AF and incubated in mouse or rat plasma at 37 °C for a period of 72 h. Release of free dolastatin was quantitated by LC/MS/MS at the indicated time points. Fig. S7 shows significantly improved stability of valine–citrulline–PABC at site A114 over site S115 in both mouse and rat plasma matrices. With SHC-D1, only 0.7% free MMAD was detected in rat plasma and 1.8% in mouse plasma after 72 h. With a longer PEG linker, HC-D1 appeared stable at site A114 in rat plasma, but was 25% cleaved when conjugated to site S115. This was also observed in mouse plasma where the level of nonspecific protease activity appeared to be in greater abundance than in rat. Complete cleavage of HC-D1 was observed after 72 h at site A114; however, similar levels of MMAD were detected after 4 h at site S115. Although SHC-D1 exhibits greater stability than HC-D1, the linker was still susceptible to MMAD release at site S115 as shown in Fig. S7. The levels of free MMAD present after 4 h in mouse plasma at site S115 with SHC-D1 was 22%, with complete degradation after 72 h. Incubation of free MMAD in mouse and rat plasma was also performed to demonstrate stability of the free dolastatin upon release. No loss or modifications were observed supporting low detection of free MMAD was due to linker stability and not through payload degradation or detection limitations of the assay. These results demonstrate that conjugation site can have a profound impact on protease cleavable linker stability, presumably by affecting steric access of the protease to the susceptible bond.

Rat Toxicology Study of NDCs. The safety profile of Her HC-A114*p*AF-NC-D1 was evaluated in male Sprague–Dawley rats. Administration of a single i.v. dose of 20, 60, or 90 mg/kg of Her HC-A114*p*AF-NC-D1 was generally well tolerated with no overt signs of toxicity. All treated rats gained weight for the duration of the study similar to vehicle control rats (Fig. S8), and there were no significant clinical observations noted for the duration of the study (14 d). On study day 5, there was a slight increase in alkaline phosphatase (ALP) in rats treated with 60 or 90 mg/kg of Her HC-A114*p*AF-NC-D1 compared with vehicle control (Table S3). These values returned to levels similar to control rats by day 14. Similar elevations in liver enzymes have been observed with thioTMAb-mpeo-DM1 (89 mg/kg or greater) and Trastuzumab-MCC-DM1 (20 mg/kg or greater) (15, 30). Minimal hematologic changes included elevated neutrophils in rats treated with 60 or 90 mg/kg Her HC-A114*p*AF-NC-D1 on study day 5 (Table S4), similar to what has previously been observed with thioTMAb-mpeo-DM1 (30). There were no additional changes in hematology or clinical chemistry values in rats treated with Her HC-A114*p*AF-NC-D1 compared with vehicle control-treated animals.

In all dose concentrations of Her HC-A114*p*AF-NC-D1 evaluated, there were pathology findings in the kidney, liver, lungs, and testes (Table S5). Test article-related findings in the kidney were primarily in the 60 and 90 mg/kg-treated animals and included interstitial inflammation, congestion, and tubular basophilia, signifying tubular regeneration. The interstitial inflammation was also observed in rats treated with 127 mg/kg of thioTMAb-mpeo-DM1 (30). In the liver, test article-related findings included dose-dependent congestion (all dose levels) and degeneration and/or necrosis (90 mg/kg only). Similar findings were also observed in rats treated with thioTMAb-mpeo-DM1 at all dose levels evaluated (47, 89, and 127 mg/kg). This finding is consistent with the increased ALP values observed at study day 5 indicative of liver injury. Dose-dependent spermatogenic degeneration was also observed in the testes of rats treated with Her HC-A114*p*AF-NC-D1. Test article-related findings in the lungs included dose-dependent congestion, alveolar edema, and increased alveolar macrophages. Similar findings were observed in rats treated with thioTMAb-mpeo-DM1 (30). Additional findings in rats treated with 60 or 90 mg/kg of Her HC-A114*p*AF-NC-D1 included subacute inflammation in the thymus and decreased lymphocytes in the thymus and spleen.

We conclude that administration of a single dose of 20, 60, or 90 mg/kg of Her HC-A114*p*AF-NC-D1 was generally well tolerated in male Sprague–Dawley rats. There were some subtle changes in hematology and clinical chemistry values (ALP and increased neutrophils) observed on day 5, which partially or completely resolved by day 14, indicative of a return to steady-state levels. In contrast to thioTMAb-mpeo-DM1 (127 mg/kg) or Transtuzumab-MCC-DM1 (50 mg/kg), there were no overt toxicology findings such as body weight loss in rats treated with Her HC-A114*p*AF-NC-D1 (15, 30). There were pathology findings observed in all dose concentrations of Her HC-A114*p*AF-NC-D1, primarily in the kidney, liver, lungs, and testes indicative of drug-induced off-target toxicity. Most findings were dose responsive with more significant effects observed in animals treated with 60 or 90 mg/kg of Her HC-A114*p*AF-NC-D1. In a separate study, using a cytotoxic drug different from MMAD, we compared the relative toxicity of NDCs vs. conventional ADCs (reduced interchain cysteine conjugates) and determined that NDCs have a superior preclinical toxicology profile in rats compared with cysteine-conjugated ADC. This will be described elsewhere.

To assess systemic exposure in the rat toxicology study, blood was sparsely sampled from 6 to 336 h. Serum was assayed for concentrations of total Ab (Ab) and for intact Ab drug conjugates (NDC).

The time vs. concentration curves illustrate that there is increased exposure with increasing dose (Fig. S9). The curves for Ab and NDC follow similar decay patterns, suggesting that the NDC is stable in the rat circulation (Fig. S9). Serum concentration values were analyzed by noncompartment analysis for pharmacokinetic parameters. The half-life, clearance, and volume of distribution remained relatively constant with increasing dose, whereas the area under the curve (AUC) and C_0 increased with increasing dose whether assayed for total Ab (Ab) or intact NDC. AUC increased in a dose-proportional manner, increasing 2.6- and 1.5-fold for a 3- and 1.5-fold increase in dose, respectively, verifying that there was systemic exposure during the toxicology study. Taken together, these data indicate that HC-A114*p*AF-NC-D1 is very stable even at the highest dose of 90 mg/kg and persists in the animal's circulation in the intact form for several weeks.

Conclusion

In summary, an expanded genetic code in CHO cells provides a robust method for the synthesis of optimized NDCs. NDCs synthesized through conjugation of SMDs with site-specifically incorporated nonnative amino acids have improved pharmaceutical properties. Compared with conventional cysteine conjugated ADCs, NDCs demonstrate superior in vitro efficacy and selectivity, in vivo pharmacokinetics and efficacy in rodent models, and more interestingly, superior efficacy in lower antigen (2+)-expressing target cells. These data support clinical evaluation of the anti-Her2 NDC (31). This approach also provided us with an opportunity to better understand how changes in conjugation site, conjugation chemistry, and stoichiometry may affect the pharmacological properties of ADCs. This further validates the emerging trend in the ADC field toward chemically defined site-specific Ab conjugates. NDCs disclosed herein are highly stable and well tolerated in rat. With the achievement of over 1 g/L Ab titers in several stable cell lines, the EuCODE platform is well positioned for next generation Ab drug development.

Materials and Methods

Nonnative Amino Acid-Containing Ab Transient Expression. CHO-S suspension-adapted cells were obtained from Invitrogen. Routine maintenance culture of CHO-S cells was performed in CHO-S FreeStyle chemical defined media (Invitrogen) supplemented with 8 mM L-glutamine (Invitrogen/Gibco). Cells were maintained according to Invitrogen's protocol. FreeStyle MAX transfection reagent was purchased from Invitrogen. The procedure of transfection was performed according to Invitrogen's FreeStyle MAX reagent protocol. The cell density was adjusted to 1×10^6 cells/mL right before transfection and the addition of *p*AF. Transfected cells were incubated at 37 °C, 8% (vol/vol) CO_2 on orbital shaker set to 125 rpm. After 7 d, the supernatant was collected for purification and the productivity of Ab was determined by IgG ELISA.

Nonnative Amino Acid-Containing Ab Stable Expression. Cells were maintained in a mixture of CD FortiCHO (Life Tech) and EX-Cell 302 (Sigma; SAFC) with GS supplement (Sigma) and 250 μM MSX (Millipore). Cells were inoculated at density of 0.3×10^6/mL in shake flask (Corning) and 5-L bioreactor (Sartorius vessel and Finess controller) on day 0. The 1 mM *p*AF was added to culture on day 5 for both shake flask and 5-L bioreactor. Ten percent (initial culture volume) of Cell Boost 5 (CB5) (HyClone) was added to culture in shake flask and bioreactor on day 5. Temperature was shifted from 37 °C to 32 °C for both shake flask and bioreactor. Additional 10% (vol/vol) CB5 was added to culture on day 7. Glucose level was monitored using NOVA Flex and additional glucose was added to culture when glucose level was below 2 g/L in culture media. Viable cell count and viability were measured by Vi-Cell instrument (Beckman Coulter). Productivity was measure by HPLC (Agilent).

ACKNOWLEDGMENTS. We thank the following Pfizer colleagues: Judy Lucas, Bryan Peano, Kenny Kim, Chris Hosselet, and LuAnna Lemon for performing all in vivo efficacy studies; Joann Wentland and Tracey Clark for bioanalytical support activities of the PK studies; Jeff Casavant and Dahui Zhou for preparation of mNC-D1 and conventional and site-specific cysteine conjugates; and Manoj Charati for preparation of A1 mc-D1 conjugate. We thank Oxford Biomedica for collaboration around the 5T4 target. We thank our Ambrx colleagues: Robin Marsden, for providing anti-MMAD Ab; Yun Bai and Joe Tuchscherer for performing Ab purification and SDS-gel analysis; Sulan Yao, Anna-Maria Putnam, and Jente Lu for assisting the preparation of figures; and Dennis Gately for conducting cell line stability studies.

1. Sapra P, Hooper AT, O'Donnell CJ, Gerber H-P (2011) Investigational antibody drug conjugates for solid tumors. *Expert Opin Investig Drugs* 20(8):1131–1149.
2. Wu AM, Senter PD (2005) Arming antibodies: Prospects and challenges for immunoconjugates. *Nat Biotechnol* 23(9):1137–1146.
3. Polakis P (2005) Arming antibodies for cancer therapy. *Curr Opin Pharmacol* 5(4): 382–387.
4. Carter PJ, Senter PD (2008) Antibody-drug conjugates for cancer therapy. *Cancer J* 14(3):154–169.
5. Hamblett KJ, et al. (2004) Effects of drug loading on the antitumor activity of a monoclonal antibody drug conjugate. *Clin Cancer Res* 10(20):7063–7070.
6. Junutula JR, et al. (2008) Site-specific conjugation of a cytotoxic drug to an antibody improves the therapeutic index. *Nat Biotechnol* 26(8):925–932.
7. Jeffrey SC, et al. (2013) A potent anti-CD70 antibody-drug conjugate combining a dimeric pyrrolobenzodiazepine drug with site-specific conjugation technology. *Bioconjug Chem* 24(7):1256–1263.
8. Strop P, et al. (2013) Location matters: Site of conjugation modulates stability and pharmacokinetics of antibody drug conjugates. *Chem Biol* 20(2):161–167.
9. Axup JY, et al. (2012) Synthesis of site-specific antibody-drug conjugates using unnatural amino acids. *Proc Natl Acad Sci USA* 109(40):16101–16106.
10. Cho H, et al. (2011) Optimized clinical performance of growth hormone with an expanded genetic code. *Proc Natl Acad Sci USA* 108(22):9060–9065.
11. Mukai T, et al. (2008) Adding l-lysine derivatives to the genetic code of mammalian cells with engineered pyrrolysyl-tRNA synthetases. *Biochem Biophys Res Commun* 371(4):818–822.
12. Ou W, et al. (2011) Site-specific protein modifications through pyrroline-carboxy-lysine residues. *Proc Natl Acad Sci USA* 108(26):10437–10442.
13. Verdier-Pinard P, Kepler JA, Pettit GR, Hamel E (2000) Sustained intracellular retention of dolastatin 10 causes its potent antimitotic activity. *Mol Pharmacol* 57(1):180–187.
14. Damelin M, et al. (2011) Delineation of a cellular hierarchy in lung cancer reveals an oncofetal antigen expressed on tumor-initiating cells. *Cancer Res* 71(12):4236–4246.
15. Lewis Phillips GD, et al. (2008) Targeting HER2-positive breast cancer with trastuzumab-DM1, an antibody-cytotoxic drug conjugate. *Cancer Res* 68(22):9280–9290.
16. Köhrer C, Sullivan EL, RajBhandary UL (2004) Complete set of orthogonal 21st aminoacyl-tRNA synthetase-amber, ochre and opal suppressor tRNA pairs: Concomitant suppression of three different termination codons in an mRNA in mammalian cells. *Nucleic Acids Res* 32(21):6200–6211.
17. Chin J, et al. (2003) An expended eukaryotic genetic code. *Science* 301:964–967.
18. Xie J, Schultz PG (2005) Adding amino acids to the genetic repertoire. *Curr Opin Chem Biol* 9(6):548–554.
19. Xu X, et al. (2011) The genomic sequence of the Chinese hamster ovary (CHO)-K1 cell line. *Nat Biotechnol* 29(8):735–741.
20. Tian F, Norman T, Chu S (2006) Hybrid suppressor tRNA for vertebrate cells. Patent publication number US20100159586.
21. Wurm FM (2004) Production of recombinant protein therapeutics in cultivated mammalian cells. *Nat Biotechnol* 22(11):1393–1398.
22. Jewett JC, Bertozzi CR (2010) Cu-free click cycloaddition reactions in chemical biology. *Chem Soc Rev* 39(4):1272–1279.
23. Doronina SO, et al. (2003) Development of potent monoclonal antibody auristatin conjugates for cancer therapy. *Nat Biotechnol* 21(7):778–784.
24. Liu C, et al. (1996) Eradication of large colon tumor xenografts by targeted delivery of maytansinoids. *Proc Natl Acad Sci USA* 93(16):8618–8623.
25. Sapra P, et al. (2013) Long-term tumor regression induced by an antibody-drug conjugate that targets 5T4, an oncofetal antigen expressed on tumor-initiating cells. *Mol Cancer Ther* 12(1):38–47.
26. Shen B-Q, et al. (2012) Conjugation site modulates the *in vivo* stability and therapeutic activity of antibody-drug conjugates. *Nat Biotechnol* 30(2):184–189.
27. Polson AG, et al. (2009) Antibody-drug conjugates for the treatment of non-Hodgkin's lymphoma: Target and linker-drug selection. *Cancer Res* 69(6):2358–2364.
28. Alley SC, et al. (2008) Contribution of linker stability to the activities of anticancer immunoconjugates. *Bioconjug Chem* 19(3):759–765.
29. Ducry L, Stump B (2010) Antibody-drug conjugates: Linking cytotoxic payloads to monoclonal antibodies. *Bioconjug Chem* 21(1):5–13.
30. Junutula JR, et al. (2010) Engineered thio-trastuzumab-DM1 conjugate with an improved therapeutic index to target human epidermal growth factor receptor 2-positive breast cancer. *Clin Cancer Res* 16(19):4769–4778.
31. Burris HA, 3rd, et al. (2011) Phase II study of the antibody drug conjugate trastuzumab-DM1 for the treatment of human epidermal growth factor receptor 2 (HER2)-positive breast cancer after prior HER2-directed therapy. *J Clin Oncol* 29(4):398–405.